



**HAL**  
open science

## Structural defects in Cu doped Bi<sub>2</sub>Te<sub>3</sub> single crystals

Jana Bludska, Ivo Jakubec, Cestmir Drasar, Petr Lostak, Jaromir Horak

► **To cite this version:**

Jana Bludska, Ivo Jakubec, Cestmir Drasar, Petr Lostak, Jaromir Horak. Structural defects in Cu doped Bi<sub>2</sub>Te<sub>3</sub> single crystals. Philosophical Magazine, 2006, 87 (02), pp.325-335. 10.1080/14786430600990337 . hal-00513772

**HAL Id: hal-00513772**

**<https://hal.science/hal-00513772>**

Submitted on 1 Sep 2010

**HAL** is a multi-disciplinary open access archive for the deposit and dissemination of scientific research documents, whether they are published or not. The documents may come from teaching and research institutions in France or abroad, or from public or private research centers.

L'archive ouverte pluridisciplinaire **HAL**, est destinée au dépôt et à la diffusion de documents scientifiques de niveau recherche, publiés ou non, émanant des établissements d'enseignement et de recherche français ou étrangers, des laboratoires publics ou privés.



**Structural defects in Cu doped Bi<sub>2</sub>Te<sub>3</sub> single crystals**

Journal:	<i>Philosophical Magazine &amp; Philosophical Magazine Letters</i>
Manuscript ID:	TPHM-05-Dec-0552.R2
Journal Selection:	Philosophical Magazine
Date Submitted by the Author:	29-Aug-2006
Complete List of Authors:	Bludska, Jana; Institute of Inorganic Chemistry, Academy of Sciences of the Czech Republic Jakubec, Ivo; Institute of Inorganic Chemistry, Academy of Sciences of the Czech Republic Drasar, Cestmir; University of Pardubice, Physics Lostak, Petr; University of Pardubice, Studentská 95, 532 10 Pardubice, Gegeral and Inorganic Chemistry Horak, Jaromir; Joint Laboratory of Solid State Chemistry of Institute of Macromolecular Chemistry, Academy of Sciences of the Czech Republic, a
Keywords:	defect structures, defects in solids
Keywords (user supplied):	tetradymite-type chalcogenides, intercalation



## Structural defects in Cu-doped Bi<sub>2</sub>Te<sub>3</sub> single crystals

By J. BLUDSKÁ<sup>†</sup>, I. JAKUBEC<sup>†</sup>, Č. DRAŠAR<sup>‡\*</sup>, P. LOŠŤÁK<sup>‡</sup>, and J. HORÁK<sup>\*\*</sup>

<sup>†</sup>Institute of Inorganic Chemistry, Academy of Sciences of the Czech Republic,  
250 68 Řež, Czech Republic

<sup>‡</sup>University of Pardubice, Čs. Legií 565, 532 10 Pardubice, Czech Republic

<sup>\*\*</sup>Joint Laboratory of Solid State Chemistry of Institute of Macromolecular Chemistry,  
Academy of Sciences of the Czech Republic, and University of Pardubice,  
Studentská 84, 530 09 Pardubice, Czech Republic

\*Corresponding author: cestmir.drasar@upce.cz

## ABSTRACT

The relation between the concentration of free charge carriers and the concentration of copper atoms in  $\text{Bi}_2\text{Te}_3$  single crystals doped with copper over a wide range of concentrations has been investigated, with the aim of clarifying the existence of inactive Cu ions. Changes in the concentration of free charge carriers arising from Cu-doping of the melt with that induced by electrochemical intercalation of copper are compared. Models of possible defect structures are proposed for both doped and intercalated single crystals of  $\text{Bi}_2\text{Te}_3$ .

## §1. INTRODUCTION

$\text{Bi}_2\text{Te}_3$  is a component of materials used in thermoelectric devices such as solid-state coolers or generators [1]. Studies of the effect of dopants on its physical properties are therefore interesting for both basic and commercial reasons. The compound is a layered semiconductor with the tetradymite structure (space group  $D_{3d}^5$ ). Its crystal structure is composed of a periodic arrangement of layers aligned perpendicular to the trigonal c-axis. Each layer is composed of five atomic planes ordered according to the following pattern:



Between  $\text{Te}^1$  atomic planes of neighbouring atoms there is a van der Waals gap.

The effects on  $\text{Bi}_2\text{Te}_3$  crystals of copper doping have been reported in numerous studies [2 – 13]; the results indicate that copper atoms embedded in the crystal structure induce a suppression of the hole concentration. Higher Cu concentration results in a crossover from hole to electron conductivity, and further increases in the Cu concentration lead to an increase in the electron concentration. A detailed analysis of the relation between the concentration of Cu atoms embedded in the crystal structure and the corresponding increase in the concentration of electrons has not yet been performed. Some authors [4, 5, 7] allege that only a fraction of the total number of copper atoms generate free electrons. According to Beckman and Bergvall [4, 5] only one-tenth of Cu atoms are electrically active, the remainder not influencing the concentration of free carriers. A similar effect was observed from studies of electrochemical intercalation of copper into a  $\text{Bi}_2\text{Te}_3$  crystal [7]. From these investigations it was concluded that approximately one-third of intercalated Cu atoms were inactive.

Intercalation as a method of doping  $\text{Bi}_2\text{Te}_3$  by copper and corresponding changes of transport coefficients linked to the occupation of the van der Waals gap by Cu ions were studied by Samaras et al. [12] and Kyratsi et al. [13]. Some authors [4, 5, 7, 10] provided

1  
2  
3 suggestions for possible ways of embedding the Cu atoms; however, the existence of  
4  
5 inactive Cu sites in the crystal structure has not yet been established. With this in mind, we  
6  
7 investigate here the relation between the concentration of free carriers and the  
8  
9 concentration of Cu atoms in the lattice. A model of possible defects in the structure of  
10  
11  $\text{Bi}_2\text{Te}_3$  crystals doped and intercalated by Cu atoms is proposed.  
12  
13  
14

## 15 16 17 §2. EXPERIMENTAL DETAILS 18

### 19 20 21 2.1. Preparation of $\text{Bi}_2\text{Te}_3$ and $\text{Bi}_2\text{Te}_3(\text{Cu})$ single crystals 22

23  
24 The starting polycrystalline samples of  $\text{Bi}_2\text{Te}_3$  and  $\text{Bi}_2\text{Te}_3(\text{Cu})$  were synthesized  
25  
26 from Bi, Cu and Te elements of 5N purity. Single crystals were grown from the melt by a  
27  
28 modified Bridgman method; the details of preparation have been reported previously by  
29  
30 Horák et al. [14]. We emphasize that copper was built into the crystals from a melt  
31  
32 containing the element. The resulting single crystals were 50-60 mm long, approximately  
33  
34 10 mm in diameter, and cleavable. Their trigonal axis  $c$  was always perpendicular to the  
35  
36 pulling direction, *i.e.* the (0001) plane was always parallel to the ampoule axis. The  
37  
38 orientation of the cleavage planes was checked using Laue back diffraction. A series of  
39  
40 crystals with various copper concentrations was synthesized and used for the preparation of  
41  
42 samples for measurements of the Hall coefficient and electrical conductivity. The  
43  
44 dimensions of a typical sample were  $0.25 \times (0.02-0.04) \times (0.6-0.8) \text{ cm}^3$ . Considering  
45  
46 experimental results obtained by Hacke [3], both the preparation of the samples and the  
47  
48 measurements were accomplished within 8 h of the single crystal being taken out of the  
49  
50 ampoule to avoid the effect of interaction of oxygen, which could influence the transport  
51  
52 coefficients. According to Hacke [3] this effect manifests itself after 10 h of exposition to  
53  
54  
55  
56  
57  
58  
59  
60

1  
2  
3 an air atmosphere. The Cu content in the  $\text{Bi}_2\text{Te}_3(\text{Cu})$  single crystals prepared from melt  
4  
5 was determined by chemical analysis.  
6  
7  
8  
9

## 10 11 12 2.2. Measurements of the Hall coefficient and electrical conductivity 13 14

15  
16 To characterize the  $\text{Bi}_2\text{Te}_3$  crystals containing various copper contents, the Hall  
17  
18 coefficient, measured with the direction of magnetic induction  $\mathbf{B}$  oriented parallel to the  
19  
20 trigonal  $\mathbf{c}$  axis,  $R_{\text{H}}(\mathbf{B}\parallel\mathbf{c})$ , and the electrical conductivity in a direction perpendicular to the  
21  
22 trigonal  $\mathbf{c}$  axis,  $\sigma_{\perp}$ , were measured at room temperature. The measurements were carried  
23  
24 out using an alternating current with a frequency of 170 Hz. Contacts were vacuum-  
25  
26 evaporated gold thin films. The electrical conductivity  $\sigma_{\perp\text{c}}$  was determined from the  
27  
28 potential drop along the sample between the voltage contacts.  
29  
30  
31  
32  
33  
34

## 35 36 2.3. Electrochemical intercalation of copper 37 38

39  
40 Samples for the preparation of copper intercalates were cleaved from  $\text{Bi}_2\text{Te}_3$  single  
41  
42 crystals. Electrodes were made by slicing perpendicular to the cleavage planes, connected  
43  
44 to a collector, and isolated by waterproof silicon rubber in a glass holder so that only the  
45  
46 desired face was exposed to the electrolyte. The geometric area of the electrodes was  
47  
48 determined from a digitized microshot.  
49

50  
51 Electrochemical intercalation was carried out in a three-electrode cell containing a  
52  
53 saturated calomel electrode (SCE) as a reference electrode, a copper wire spiral as an  
54  
55 auxiliary electrode and a 0.1 M aqueous solution of copper sulphate as an electrolyte. A  
56  
57 potentiostat (PAR model 263) controlled by computer was used for the experiments, which  
58  
59 were performed at room temperature. Electrochemical intercalation of copper into  $\text{Bi}_2\text{Te}_3$   
60

sample was carried out in the following way. A constant current of  $20 \mu\text{A}$  ( $i = 80 \mu\text{A cm}^{-2}$ ) was passed through a  $\text{Bi}_2\text{Te}_3$  electrode and the cathode potential was recorded with time for 11 days. This time period was optimized on the basis of our preliminary experiments. Longer time of intercalation leading to higher Cu content in the  $\text{Bi}_2\text{Te}_3$  host crystal, leads to exfoliation of the layered crystal. The copper concentration in the  $\text{Cu}_x\text{Bi}_2\text{Te}_3$  crystal was calculated from the charge passed through the crystal.

### §3. RESULTS

Results of the measurements of Hall coefficient and electrical conductivity as a function of the concentration of Cu atoms incorporated in the crystal structure,  $n_{\text{Cu}}$ , are listed in Table 1 and depicted in figure 1. Since all the studied samples are close to the intrinsic regime, we used a two-carrier model to determine the free carrier concentration. In this case, the Hall coefficient is given in terms of the concentrations of holes  $p$  and electrons  $n$  by

$$R_H = \frac{3\pi}{8} \cdot \frac{p \cdot \mu_p^2 - n \cdot \mu_n^2}{e(p \cdot \mu_p + n \cdot \mu_n)^2}, \quad (1)$$

where  $\mu_p$  and  $\mu_n$  are the mobility of holes and electrons, respectively. To make use of equation (1) one needs the intrinsic concentration  $n_i$ , which relates  $n$  and  $p$  ( $n_i^2 = n \cdot p$ ), and  $\mu_p$  and  $\mu_n$  of the host material. We found  $n_i^2 = 1.5 \times 10^{36} \text{ cm}^{-6}$  and  $\mu_p = 450$ ,  $\mu_n = 1250 \text{ cm}^2\text{s}^{-1}\text{V}^{-1}$  in the literature [2]. The magnitudes of mobility characterize "pure"  $\text{Bi}_2\text{Te}_3$  and since these values are supposed to be affected at samples with higher content of Cu we confine our calculations to samples 1-6 only. The concentrations of free carriers are given in Table 1. The dependence of electrode potential



on copper content is shown in figure 3. The intercalate complements the samples prepared from the melt.

#### §4. DISCUSSION

From the parameters in Table 1, it is evident that Cu suppresses the concentration of holes in  $\text{Bi}_2\text{Te}_3$ . Interstitially incorporated Cu accounts for the observed decrease of hole concentration. Accordingly, one Cu atom should produce one electron compensating a hole. However, the number of electrons produced per Cu atom is less than 1 and decreases with Cu content (the parameter of interest is  $n/n_{\text{Cu}}$  in Table 2), i.e. the doping efficiency of Cu decreases with Cu content.

In order to describe the observed effect, we need to determine the native defect concentration in undoped  $\text{Bi}_2\text{Te}_3$ . The formation of native defects and their concentration is in close relation with the overstoichiometry of Bi atoms in  $\text{Bi}_2\text{Te}_3$  single crystals prepared from a stoichiometric melt. The presence of excess Bi atoms can induce the creation of the following defects:

- a) vacancies in the tellurium sublattice ( $V_{\text{Te}}^{+2}$ ) carrying two positive charges,
- b) anti-site (AS) defects ( $\text{Bi}_{\text{Te}}^{-1}$ ) carrying one negative charge,
- c) structural defects, e.g.  $\text{Bi}_3\text{Te}_4^{-1}$ ,  $\text{Bi}_4\text{Te}_5^{-1}$ ; it should be mentioned that these defects correspond - as to their charge - to AS defects  $\text{Bi}_{\text{Te}}^{-1}$ .

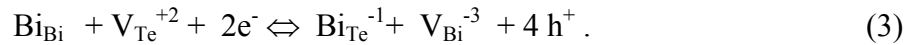
And we also have to acknowledge the presence of

- d) vacancies in the bismuth sublattice ( $V_{\text{Bi}}^{-3}$ ), which are believed to carry three negative charges [15].

The model is characterized by the idea that overstoichiometric Bi atoms -  $\text{Bi}_{\text{over}}$  - enter both the cation sublattice (on regular sites such as  $\text{Bi}_{\text{Bi}}$ ) as well as the anion sublattice as AS defects ( $\text{Bi}_{\text{Te}}^{-1}$ ). This process can be expressed by the following equation

$$a \text{Bi}_{\text{over}} + b (\text{V}_{\text{Bi}} + 1.5\text{V}_{\text{Te}}) = b \text{Bi}_{\text{Bi}} + (a-b) \text{Bi}_{\text{Te}}^{-1} + ((5/2)b-a) \text{V}_{\text{Te}}^{+2} + (3a-6b) h^+. \quad (2)$$

Hence, the defect structure of  $\text{Bi}_2\text{Te}_3$  ranks among hybrids of Schottky and antistructure disorder [16]. One can describe the process of creation and interaction of native defects by an equilibrium equation respecting charge neutrality



We note that a similar model for native defects in  $\text{Sb}_2\text{Te}_3$  was used by Horak [17].

According to eq.3, part of the  $\text{Bi}_{\text{over}}$  atoms occupy sites in the anion sublattice at  $\text{Te}^2$ -sites and the formation of each AS defect is accompanied by the formation of a cation vacancy  $\text{V}_{\text{Bi}}^{-3}$ . Furthermore this model satisfies the condition that the ratio of the number of cation sublattice sites to anion sublattice ones is equal to 2/3. Also, it follows from eq.3 that the number of incorporated overstoichiometric  $\text{Bi}_{\text{over}}$  atoms influences the concentration of free carriers. In this model we do not concede the existence of Bi atoms at interstitial sites or inside the van der Walls gap.

The above-mentioned conditions characterizing the model are determined by the following relations:

- a)  $[\text{Bi}_{\text{over}}] = [\text{Bi}_{\text{Bi}}] + [\text{Bi}_{\text{Te}}^{-1}]$  (mass balance)
- b)  $[\text{Bi}_{\text{Te}}^{-1}] = [\text{V}_{\text{Bi}}^{-3}]$  (see eq.3)
- c)  $2 [\text{V}_{\text{Te}}^{+2}] + [h^+] = [\text{Bi}_{\text{Te}}^{-1}]$  (charge balance)
- d)  $[\text{Bi}_{\text{Bi}}] / ([\text{V}_{\text{Te}}^{+2}] + [\text{Bi}_{\text{Te}}^{-1}]) = 2/3$  (stoichiometry) (4a,b,c,d)

The following concentrations of point defects were calculated using relations (4a,b,c,d), the measured hole concentration  $[h^+] = 7.65 \times 10^{18} \text{ cm}^{-3}$  ( $[h^+] = p$ ) in undoped  $\text{Bi}_2\text{Te}_3$  and the value of  $[\text{Bi}_{\text{over}}] = 3.1 \times 10^{19} \text{ cm}^{-3}$  taken from [18]:

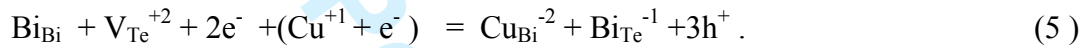
$$[\text{V}_{\text{Bi}}^{-3}] = 1.68 \times 10^{19} \text{ cm}^{-3}, [\text{V}_{\text{Te}}^{+2}] = 2.98 \times 10^{19} \text{ cm}^{-3}, [\text{Bi}_{\text{Te}}^{-1}] = 1.68 \times 10^{19} \text{ cm}^{-3} \text{ and}$$

$$[\text{Bi}_{\text{Bi}}] = 1.42 \times 10^{19} \text{ cm}^{-3}.$$

It should be noted that with respect to the validity of the charge neutrality relation

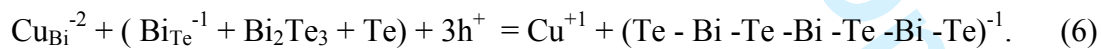
$$(2V_{\text{Bi}}^{-3} + 3V_{\text{Te}}^{+2}) = 0, \text{ only } 4.6 \times 10^{18} \text{ cm}^{-3} \text{ of } [V_{\text{Te}}^{+2}] \text{ sites are electrically active.}$$

Knowledge of the nature and concentration of native defects in undoped  $\text{Bi}_2\text{Te}_3$  allow us to explain an experimentally observed effect – the apparent occurrence of electrically inactive Cu atoms in the crystal structure. We suppose that next to interstitial Cu there is another way of incorporating Cu atoms that can be described by the following equation:

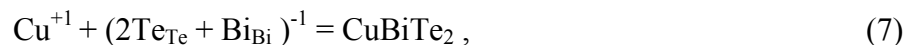


The equation indicates that incorporation of Cu induces a shift of equilibrium in favour of antisite defects, changing the free carrier concentration to six holes per one Cu atom. Hence, incorporation of Cu shifts the Bi atom from the cation sublattice to the anion sublattice. This process alone is associated with the formation of four holes.

A crossover of an antisite defect  $\text{Bi}_{\text{Te}}^{-1}$  from a five-layer to a seven-layer lamella can be described by the equation  $\text{Bi}_{\text{Te}}^{-1} + \text{Bi}_2\text{Te}_3 + \text{Te} = \text{Bi}_3\text{Te}_4^{-1}$ . Note that concerning the charge, an antisite defect corresponds to lamella  $\text{Bi}_3\text{Te}_4^{-1}$  with delocalized electrons. This process, including copper, can be expressed by the following equations:



$\text{Cu}^{+1}$  ion reacts with the remainder of the five-layer lamella (e.g.  $+2\text{Te}_{\text{Te}} + \text{Bi}_{\text{Bi}}$ ) and forms a new lamella  $\text{CuBiTe}_2$ :



Both structures  $\text{CuBiTe}_2$  and  $\text{Bi}_3\text{Te}_4^{-1}$  belong to the same space group as the host  $\text{Bi}_2\text{Te}_3$  -  $D_{3d}^5$  [19], [20].

In summary we have two ways for the incorporation of copper in  $\text{Bi}_2\text{Te}_3$ :

- 1  
2  
3 a) one connected with formation of lamellae  $[\text{CuBiTe}_2 + \text{Bi}_3\text{Te}_4^{-1}]^{-1}$  (compensated by  
4 holes),  
5  
6  
7  
8 b) the other connected with formation of interstitial  $\text{Cu}_i^+$  (compensated by electrons).  
9

10  
11  
12 The coexistence of both processes, which compensate each other, accounts for the low  
13 doping efficiency of Cu in  $\text{Bi}_2\text{Te}_3$ .  
14

15  
16  
17 The formation of the lamellae is corroborated by results in references [21, 22].  
18 According to these papers incorporation of Me dopant (Me = Ge, Sn, Pb) into  $\text{Bi}_2\text{Te}_3$  single  
19 crystal enables the formation of seven-layer lamellae of  $\text{MeBi}_2\text{Te}_4$  type. In these lamellae,  
20 Me atoms are supposed to be in a formal 2+ oxidation state. In these electrically neutral  
21 seven-layer lamellae, the atomic planes are ordered as follows:  
22 (Te–Bi–Te–Me–Te–Bi–Te). Such a lamella carries no charge and corresponds to a  
23 defined compound of the  $D_{3d}^5$  space group as host lattice. However, it has to be noted that  
24 the formation of uncharged seven-layer lamella of  $\text{GeBi}_2\text{Te}_4$ -type prepared by heat  
25 treatment of a mixture of  $\text{Bi}_2\text{Ge}_x\text{Te}_3$  ( $x = 0.2\text{--}0.4$ ) stoichiometry, as confirmed by  
26 crystallographic and high-resolution electron microscopy methods [21, 22], is connected,  
27 owing to the tellurium deficiency, with the formation of seven-layer lamella of the type  
28 (Te–Bi–Te–Bi–Te–Bi–Te)<sup>-1</sup>.  
29  
30  
31  
32  
33  
34  
35  
36  
37  
38  
39  
40  
41  
42  
43  
44  
45  
46

47 This model allow us, as a side effect, to determine the concentration of Cu donors  
48 ( $\text{Cu}_i^+$ ),  $\text{CuBiTe}_2$  lamellae, and  $(\text{Bi}_3\text{Te}_4)^{-1}$  lamellae using the following equations:  
49

$$50 \quad n_{\text{Cu}} = [\text{Cu}_i^+] + [\text{CuBiTe}_2] \quad \text{and} \quad (8)$$

$$51 \quad n = [\text{Cu}_i^+] - [\text{CuBiTe}_2], \quad (9)$$

52 where  $n_{\text{Cu}}$  is the total concentration of copper. Though, it is not possible to compute the  
53 concentrations of free carriers and defects exactly we summarize some approximate results  
54 in Table 2. The concentrations of some defects as a function of  $n_{\text{Cu}}$  are also shown in figure  
55  
56  
57  
58  
59  
60

1  
2  
3 2. The results support the models for the incorporation of copper. We observe a decreasing  
4 doping efficiency with increasing concentration of Cu indicating a progressive rising  
5 influence of  $(\text{Bi}_3\text{Te}_4)^-$  defects. Hence the charge competition between  $\text{Cu}_i^+$  and  $(\text{Bi}_3\text{Te}_4)^-$   
6 accounts for the apparent existence of inactive copper.  
7  
8  
9  
10  
11

#### 12 13 14 15 4.2. Structural defects in intercalated $\text{Cu}_x\text{Bi}_2\text{Te}_3$ crystals

16  
17  
18 In addition to the investigation of the concentration of active copper atoms in  
19  $\text{Bi}_2\text{Te}_3$  (Cu) crystals grown from the melt, the nature of Cu atoms intercalated into the host  
20 crystal from solution was also studied.  
21  
22  
23

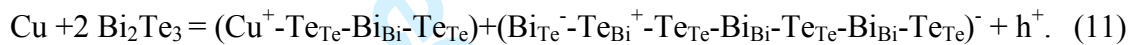
24  
25 From the dependence of  $E$  vs.  $n_{\text{Cu}}$ , where  $E$  is cathode potential and  $n_{\text{Cu}}$  is total  
26 concentration of intercalated copper, it can be concluded that a minimum separates the  
27 regions of hole from electron conductivity (see figure 3). In the minimum the total charge  
28 of acceptors relevant to the host p- $\text{Bi}_2\text{Te}_3$  is just compensated by Cu donors embedded in  
29 the intercalate. The concentration of donors,  $[\text{Cu}_i^+]$ , depends on the total concentration of  
30 embedded Cu atoms,  $n_{\text{Cu}}$ , and on the concentration of inactive Cu in four-layer lamellae:  
31  
32  
33  
34  
35  
36  
37  
38  
39

$$40 \quad [\text{Cu}^+] = n_{\text{Cu}} - [\text{CuBiTe}_2]. \quad (10)$$

41  
42  
43 If the investigated crystal ( $V = 0.17 \text{ cm}^3$ ), say, contains  $1.22 \times 10^{18}$  (=square root of  $n_i^2$ )  
44 acceptors, approximately the same number of donors must be active. However, from our  
45 experiment it follows that the position of the minimum in the function  $E(n_{\text{Cu}})$  corresponds  
46 to  $\approx 1.9 \times 10^{18}$  Cu atoms. This result suggests that only about 64% embedded  $\text{Cu}^+$ - ions  
47 generate free electrons, which is in good agreement with results obtained by McCarty and  
48 Goldsmid [7], who stated that one intercalated Cu atom generates 0.65 of an electron. In  
49 our opinion, the observed effect can be well explained by the formation of  $\text{CuBiTe}_2$  and  
50  $(\text{Bi}_3\text{Te}_4)^-$  lamellae. Providing each Cu atom liberates an electron of higher mobility  
51  
52  
53  
54  
55  
56  
57  
58  
59  
60

1  
2  
3 compared to that of a hole, one needs fewer electrons to accomplish the p to n crossover of  
4 conductivity type. However we observe the opposite trend.  
5  
6

7  
8 Though changes in the concentrations of free carriers are the same for both Cu  
9 doping from the melt and Cu intercalation, it is probable that the embedding of Cu atoms  
10 into each does not result in the formation of the same lamellae structures. When the crystal  
11 is grown from the melt we assume the formation of seven-layer lamellae with a  
12 symmetrical structure of (Te-Bi-Te-Bi-Te-Bi-Te)<sup>-</sup> type; such a symmetrical lamella can  
13 never arise if copper is intercalated into the van der Waals gap. For reasons given below an  
14 anomaly in the ordering of atomic planes in a seven-layer lamella should be considered:  
15  
16  
17  
18  
19  
20  
21  
22  
23



25  
26  
27  
28 Our model of the formation of (Cu BiTe<sub>2</sub>) and (Bi<sub>3</sub>Te<sub>4</sub>)<sup>-</sup> lamellae in an intercalated crystal  
29 involves the following steps:  
30  
31  
32

33 An embedding of Cu<sup>+</sup> ion into the van der Waals gap of the crystal leads to a  
34 splitting of one Te-Bi-Te-Bi-Te five-layer lamella and formation of a CuBiTe<sub>2</sub> structure;  
35 the remainder of the original lamella, *i.e.* Bi-Te atomic planes, interact with another five-  
36 layer lamella giving rise to an asymmetric seven-layer lamella with a delocalized electron.  
37  
38 The occurrence of the asymmetric seven-layer lamella arising as a result of electrochemical  
39 intercalation, *i.e.* the assumed alteration of Bi and Te positions in the formula (see equation  
40 11), is acceptable, since the formation of Bi<sub>Te</sub><sup>-</sup> -type defects was confirmed by Miller [23]  
41 and Hulliger [24]. The formation of Te-Te bonds in bismuth telluride synthesized under  
42 pressure was reported by Atabaeva [25]. From our previous experiments, it followed that,  
43 in the course of intercalation of copper into the van der Waals gap, Te<sup>1</sup>-Te<sup>1</sup> atomic planes  
44 are opened and considerable pressure occurs within a resin mantle where the electrode is  
45 fixed. An increasing pressure accompanying the embedding of Cu atoms into the van der  
46  
47  
48  
49  
50  
51  
52  
53  
54  
55  
56  
57  
58  
59  
60

1  
2  
3 Waals gaps was reported by Korzhuev as a reason for an increase in the lattice parameter  $c$   
4  
5 [26].  
6  
7

8  
9 The model allowing the occurrence of active and inactive copper atoms intercalated  
10 into the  $\text{Bi}_2\text{Te}_3$  crystals is also supported by results of cyclic voltammetry [27]; it was  
11 shown in these studies that only 60% of the total number of intercalated Cu atoms can be  
12 released from the crystal during the subsequent deintercalation; *i.e.* 40% of intercalated  
13 copper ions remain embedded in the crystal.  
14  
15  
16  
17  
18  
19

#### 20 21 22 23 §4. CONCLUSIONS 24

25 The relation between the concentration of free charge carriers and that of embedded copper  
26 atoms has been studied in Cu-doped  $\text{Bi}_2\text{Te}_3$  and compared with those resulting from  
27 electrochemical intercalation. A model of defect structures arising from Cu doping or  
28 intercalation in tetradymite-type  $\text{Bi}_2\text{Te}_3$  single crystals is proposed to clarify the occurrence  
29 of inactive embedded copper ions. The inactive copper can be explained in terms of the  
30 formation of electrically neutral four-layer lamellae containing univalent copper, which  
31 matches the structure of the host material. The formation of these lamellae is accompanied  
32 by the formation of seven-layer lamellae carrying delocalized negative charges  
33 compensated by free holes. With respect to different mechanisms of embedding, we  
34 assume different stacking of seven-layer lamellae in doped and intercalated crystals.  
35  
36  
37  
38  
39  
40  
41  
42  
43  
44  
45  
46  
47  
48  
49  
50  
51  
52  
53

#### 54 55 **Acknowledgements** 56

57 The financial support of the Academy of Sciences of the Czech Republic (Research Plan  
58 AV0Z40320502), the Ministry of Education, and Youth and Sports (project MSM  
59 0021627501 and project LC523) is gratefully acknowledged.  
60

1  
2  
3  
4  
5  
6  
7  
8  
9  
10  
11  
12  
13  
14  
15  
16  
17  
18  
19  
20  
21  
22  
23  
24  
25  
26  
27  
28  
29  
30  
31  
32  
33  
34  
35  
36  
37  
38  
39  
40  
41  
42  
43  
44  
45  
46  
47  
48  
49  
50  
51  
52  
53  
54  
55  
56  
57  
58  
59  
60

For Peer Review Only



## References

- [1] H. Scherrer and S. Scherrer, in *Bismuth telluride, antimony telluride, and theirs solutions*, CRC Handbook of Thermoelectrics, edited by D. M. Rowe (New York, London, Tokyo: CRS Press, Boca Raton 1995), p. 211.
- [2] K. Weiss, P. Fielding and F. A Kroeger, *Z. Phys. Chem., Suppl. Heft (N. F.)* **26**, 145 (1960).
- [3] G. Hacke, *Z. angew. Phys.* **14** 102 (1962).
- [4] O. Beckman and P. Bergvall, *Ark. Fys.* **24** 113 (1963).
- [5] O. Beckman and P. Bergvall, *Ark. Fys.* **28** 215 (1964).
- [6] R. O. Carlson, *J. Phys. Chem. Solids* **13** 65 (1968).
- [7] T. A. McCarty and H. J. Goldsmid, *J. Phys., D, Appl. Phys.* **3** 697 (1970).
- [8] T. A. McCarty and H. J. Goldsmid, *Energy Convers.* **10** 125 (1970).
- [9] H. Sussmann and K. Loof, *Phys. Status Solidi, A - Appl. Res.* **37** 467 (1976).
- [10] M. A. Korzhuev and T. E. Svechnikova, *Fiz. Tverd. Tela* **34** 492 (1992).
- [11] J. B. MacLachlan, W. H. Kruesi and D. J. Fray, *J. Mater. Sci.* **27** 4223 (1992).
- [12] I. Samaras, E. Hatzikraniotis, K.M. Paraskevopoulos, *et al.*, paper presented at the 10<sup>th</sup> Greek Conference in Solid State Physics, Delfi, Greece, 18-21 Sept.
- [13] Th. Kyratsi, E. Hatzikraniotis, K. M. Paraskevopoulos, *et al.*, *Ionics* **3** 305 (1997).
- [14] J. Horák, P. Lošťák and J. Guerts, *Phys. Status Solidi, B - BasicRes.* **167** 459 (1991).
- [15] P. Pecheur and J. Toussaint, *Phys. Chem. Solids* **55** 327 (1984).

- 1  
2  
3 [16] F.A.Kroeger, 1974, *The Chemistry of imperfect crystals*, North-Holland publishing  
4 company-Amsterdam-Oxford , p. 244  
5  
6  
7  
8 [17] J.Horak,P. Lošťák, Č. Drašar, J.S. Dyck, Z. Zhou, C.Uher, , *J.Solid StatChem.*,**178**,  
9  
10 2907 (2005)  
11  
12  
13 [18] G.Offergeld, and J. van Cakenberghe, *J. Phys. Chem. Solids* **11** 310 (1959)  
14  
15  
16 [19] F. Hulliger, *Structural Chemistry of Layer-Type Phases*, ed. by F. Lévy, Dordrecht  
17 Holland/Boston U.S.A., D. Riedel Publishing Company, p. 75.  
18  
19  
20  
21 [20] PDF 38 – 458, Joint Committee on Powder Diffraction Standards, International  
22 Center for Diffraction Data, Swarthmore, P.A.  
23  
24  
25  
26  
27 [21] N. Frangis, S. Kuypers, C. J. Manolikas, *et al.*, *Solid State Commun.* **69** 817 (1989).  
28  
29  
30 [22] N. Frangis, S. Kuypers, C. J. Manolikas, *et al.*, *J. Solid State Chem.* **84** 314 (1990).  
31  
32  
33 [23] G. R. Miller and Li Che-Yu, *J. Phys. Chem. Solids* **26** 173 (1956).  
34  
35  
36 [24] F. Hulliger, in *Structural Chemistry of Layer-Type Phases*, edited by F. Lévy  
37 (Dordrecht Holland /Boston U.S.A., D. Reidel Publishing Company, 1976), p.517.  
38  
39  
40  
41 [25] E. Ya Atabaeva, E. S. Itskevich, S. A. Mashkov, *et al.*, *Sov. Phys.- Solid State* **10**  
42 4323 (1968).  
43  
44  
45  
46 [26] M. A. Korzhuev, S. N. Chizhevskaya, T. E. Svechnikova, *et al.*, *Neorg.Mater.* **28** 1383  
47 (1992).  
48  
49  
50  
51  
52 [27] J. Bludská, S. Karamazov, J. Navrátil, *et al.*, *Solid State Ionics* **171** 254 (2004).  
53  
54  
55  
56  
57  
58  
59  
60

1  
2  
3  
4  
5  
6  
7 **Captions of figures**  
8  
9

10 **figure 1**

11 Hall coefficient and electrical conductivity of Cu-doped  $\text{Bi}_2\text{Te}_3$  as a function of  
12 concentration of Cu (single crystals prepared from melt).  
13  
14

15  
16  
17 **figure 2**

18 Concentration of holes  $[\text{h}^+]$ , four-layer lamellae  $[\text{CuBiTe}_2]$  and interstitial  $[\text{Cu}_i^+]$  as a  
19 function of Cu concentration  $n_{\text{Cu}}$ .  
20  
21

22  
23  
24 **figure 3**

25 Dependence of electrode potential on the copper concentration in  $\text{Cu}_x\text{Bi}_2\text{Te}_3$  single crystal  
26  $E$  = electrode potential vs. SCE,  $n_{\text{Cu}}$  = total concentration of Cu atoms.  
27  
28  
29  
30  
31  
32  
33  
34  
35  
36  
37  
38  
39  
40  
41  
42  
43  
44  
45  
46  
47  
48  
49  
50  
51  
52  
53  
54  
55  
56  
57  
58  
59  
60

**Table 1**

Hall constant, electrical conductivity and concentration of free charge carriers as a function of Cu concentration. Since higher concentrations of Cu are supposed to affect the mobility of carriers the free carrier concentrations of samples with highest content of Cu are not listed due to probable inaccuracy.

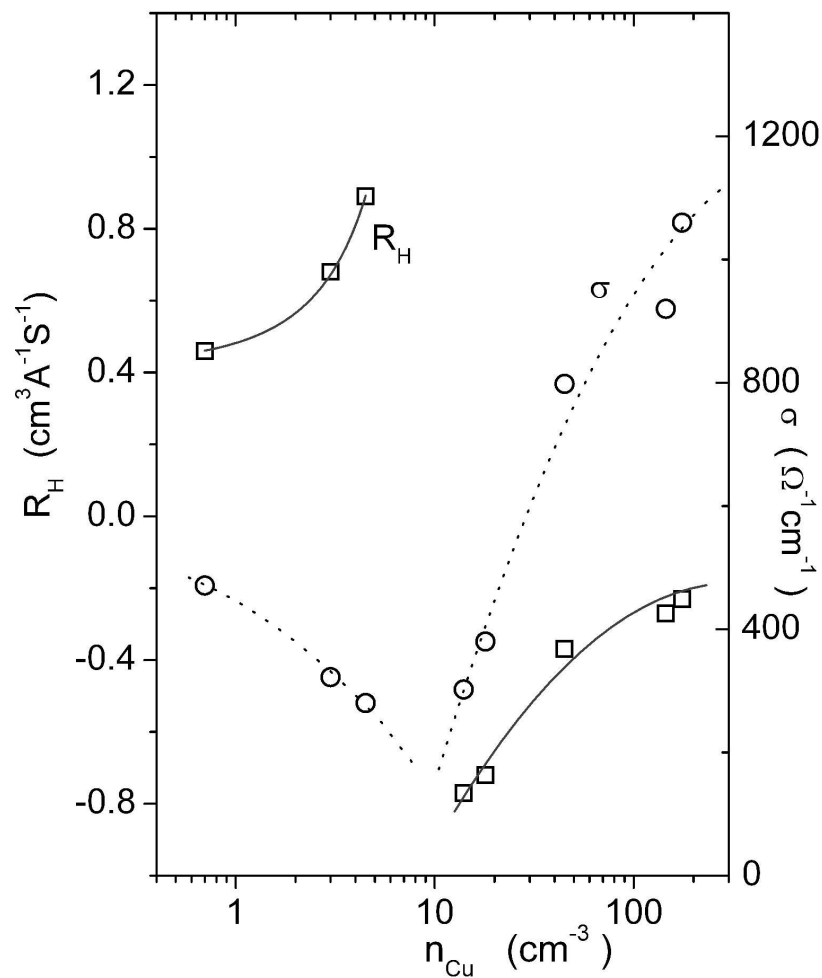
Sample	$n_{\text{Cu}}$ ( $10^{18}\text{cm}^{-3}$ )	$R_{\text{H}}(\text{B}\parallel\text{c})$ ( $\text{cm}^3\text{A}^{-1}\text{s}^{-1}$ )	$\sigma_{\perp}$ ( $\Omega^{-1}\text{cm}^{-1}$ )	[n] ( $10^{17}\text{cm}^{-3}$ )	[h] ( $10^{18}\text{cm}^{-3}$ )
1	0.0	0.42	526	1.96	7.65
2	0.7	0.46	471	2.05	7.31
3	3.0	0.68	322	2.10	7.14
4	4.5	0.89	280	2.22	6.75
5	14.0	-0.77	302	5.20	2.88
6	18.0	-0.72	380	5.00	3.00
7	45.0	-0.37	798		
8	145.0	-0.27	920		
9	175.0	-0.23	1060		

**Table 2**

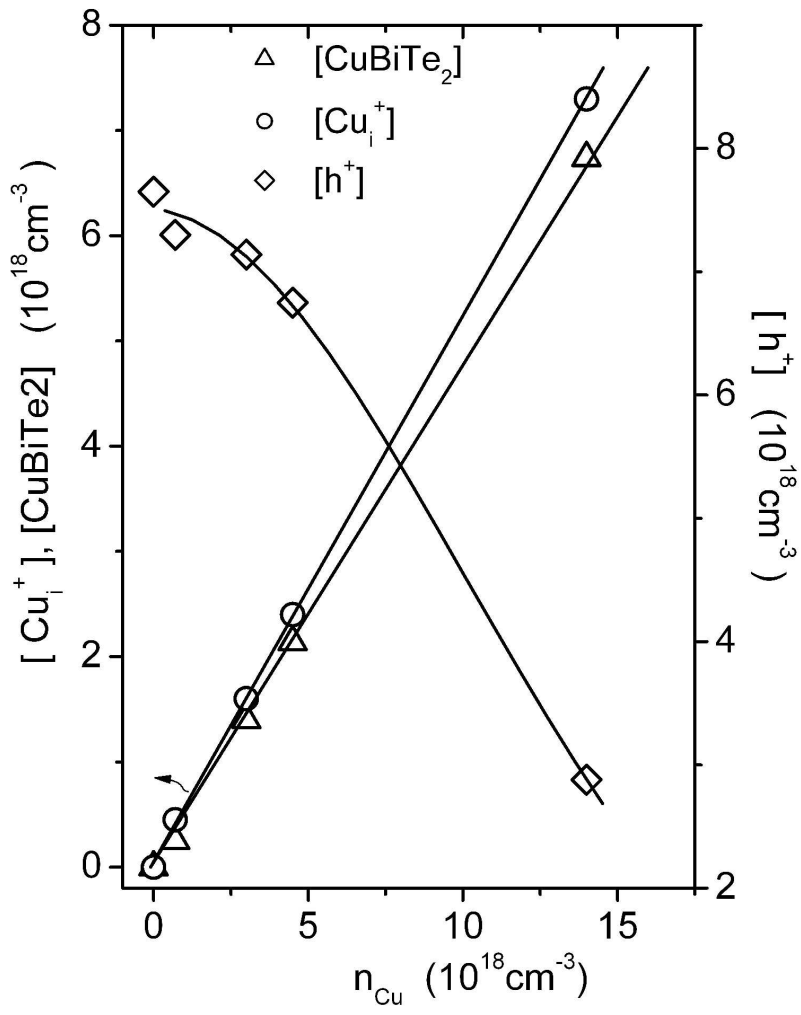
Concentrations of electrons, Cu donors [ $\text{Cu}_i^{+1}$ ], four-layer lamellae [ $\text{CuBiTe}_2$ ], seven-layer lamellae [ $\text{Bi}_3\text{Te}_4^{-1}$ ] and the ratio [n]/ $n_{\text{Cu}}$  as a function of Cu.

Sample	$n_{\text{Cu}}$ ( $10^{18}\text{cm}^{-3}$ )	[n] ( $10^{17}\text{cm}^{-3}$ )	$[\text{Cu}_i^{+1}]$ ( $10^{18}\text{cm}^{-3}$ )	$[\text{CuBiTe}_2]$ ( $10^{18}\text{cm}^{-3}$ )	$\text{Bi}_3\text{Te}_4^{-1}$ ( $10^{18}\text{cm}^{-3}$ )	[n]/ $n_{\text{Cu}}$ (-)
1	0.0	1.96	0	0	0	-
2	0.7	2.05	0.45	0.25	0.25	0.29
3	3.0	2.10	1.60	1.40	1.40	0.071
4	4.5	2.22	2.36	2.14	2.14	0.049
5	14.0	5.20	5.20	6.74	6.74	0.037
6	18.0	5.00	9.03	8.98	8.98	0.028

1  
2  
3  
4  
5  
6  
7  
8  
9  
10  
11  
12  
13  
14  
15  
16  
17  
18  
19  
20  
21  
22  
23  
24  
25  
26  
27  
28  
29  
30  
31  
32  
33  
34  
35  
36  
37  
38  
39  
40  
41  
42  
43  
44  
45  
46  
47  
48  
49  
50  
51  
52  
53  
54  
55  
56  
57  
58  
59  
60



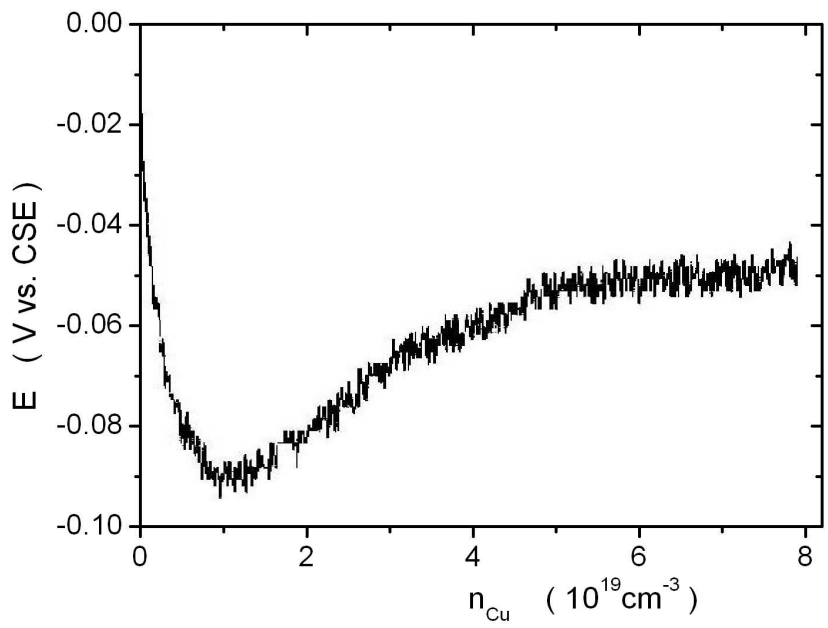
191x274mm (630 x 630 DPI)



191x274mm (630 x 630 DPI)

1  
2  
3  
4  
5  
6  
7  
8  
9  
10  
11  
12  
13  
14  
15  
16  
17  
18  
19  
20  
21  
22  
23  
24  
25  
26  
27  
28  
29  
30  
31  
32  
33  
34  
35  
36  
37  
38  
39  
40  
41  
42  
43  
44  
45  
46  
47  
48  
49  
50  
51  
52  
53  
54  
55  
56  
57  
58  
59  
60

1  
2  
3  
4  
5  
6  
7  
8  
9  
10  
11  
12  
13  
14  
15  
16  
17  
18  
19  
20  
21  
22  
23  
24  
25  
26  
27  
28  
29  
30  
31  
32  
33  
34  
35  
36  
37  
38  
39  
40  
41  
42  
43  
44  
45  
46  
47  
48  
49  
50  
51  
52  
53  
54  
55  
56  
57  
58  
59  
60



288x201mm (150 x 150 DPI)

View Only